Enhanced two-photon processes in single quantum dots inside photonic crystal nanocavities

Ziliang Lin* and Jelena Vučković
E. L. Ginzton Laboratory, Stanford University, Stanford, California 94305, USA
(Received 9 November 2009; published 5 January 2010)

We show that the two-photon transition rates of quantum dots coupled to nanocavities are enhanced by up to several orders of magnitude relative to quantum dots in bulk host. We then propose how to take advantage of this enhancement to implement coherent quantum-dot excitation by two-photon absorption, entangled photon pair generation by two-photon spontaneous emission, and single-photon generation at telecom wavelengths by two-photon stimulated and spontaneous emission.

DOI: 10.1103/PhysRevB.81.035301 PACS number(s): 42.50.−p

I. INTRODUCTION

Recent studies of semiconductor quantum dots (QDs) coupled to photonic crystal (PC) cavities have shown their potential for quantum-information science. Experiments have demonstrated creation of single photons in the near infrared,[1,2] Purcell enhancement of QD spontaneous emission rates,[3] and polariton state splitting in strong-coupling regime.[4–6] However, many important challenges remain in the QD-PC cavity systems. Among them is the generation of indistinguishable single photons, preferably at telecom wavelengths. This challenge results from the fact that a single incoherently excited QD has to undergo phonon-assisted relaxation to its lowest excited state so the emitted single photons have different temporal profiles.[7,8] For this reason, the maximum demonstrated indistinguishability between photons emitted from a single incoherently excited QD has been around 81%.[9] This problem would be resolved by exciting QDs directly on resonance and 90% indistinguishability has been recently reported from such a system in a micropillar cavity.[10] Coherent excitation is also of great interest for quantum-information science because it also enables manipulation of QD states. However, this type of excitation experiments face the difficulty of separating signal and probe photons that have the same wavelength and are thus constrained in terms of cavity geometry and strength of resulting cavity QED effects. Another challenge for the QD-PC cavity system is the generation of entangled photon pairs.[11] Although photon pairs can be created from biexciton decay cascade in a QD, the pairs are not entangled in polarization because the intermediate exciton states are split by anisotropic electron-hole exchange interactions,[12,13] which has to be compensated in order to recover entanglement.[14,15]

Two-photon absorption (TPA) and Two-photon emission (TPE) in QDs coupled to PC cavities can solve these challenges. TPA allows coherent excitation of the QDs when the frequencies of the two photons are tuned such that their sum matches the transition frequency of the QDs and at the same time allows for the frequency separation of the signal and probe photons. On the other hand, TPE from an excited QD allows the generation of entangled photon pairs on demand at telecom wavelengths. Recently, TPE in both optically pumped bulk GaAs and electrically pumped GaInP/AlGaInP quantum wells have been demonstrated.[16] However, TPE in QDs has not been observed so far because two-photon transition rates are much slower than single-photon rates as the former involve virtual intermediate states. For the same reason, a typical QD TPA experiment requires an ensemble of QDs as well as pulsed laser to provide enough excitation power.[17,18]

Here, we propose to use PC cavities to enhance the TPA and TPE rates in a single QD (Fig. 1). We show that such enhancement leads to significant reduction in the two-photon excitation power requirement so that continuous-wave lasers are sufficient for exciting a single QD. At the same time, the enhancement makes QD-PC cavity systems a promising candidate for observing TPE from a single QD and for generating entangled photons by this process. These effects have not been studied in atom-cavity systems so far because they typically exhibit much smaller Purcell factors and similarly much smaller enhancements of two-photon processes.

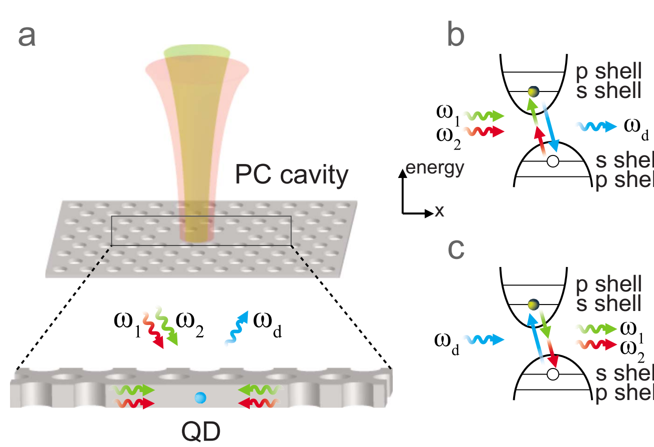

FIG. 1. (Color online) (a) Setup for enhanced two-photon absorption experiment: two laser beams with frequencies ω_1 and ω_2 are injected to a double-mode cavity. (b) Enhanced two-photon absorption and single-photon generation in a QD with a lateral electric field applied to it in the lateral x direction. The lateral electric field shifts apart the hole valence band and the electron conduction band and therefore breaks the parity selection rule. (c) Enhanced two-photon spontaneous emission in a QD as a reverse process of two-photon absorption. The one-photon excited electron recombines with the hole and generates entangled photon pair via two-photon spontaneous emission.

II. THEORETICAL ANALYSIS

A. Two-photon absorption

We first consider the case of TPA: the QD is excited from a ground state with frequency ω_g to an excited state with frequency $\omega_e=\omega_g+\omega_d$ by two photons of frequencies ω_1 and ω_2 [Fig. 1(b)]. According to time-dependent perturbation theory,[19] the transition rate for this process is $\gamma^{\mathrm{TPA}}=2\pi|\Omega_{\mathrm{eff}}|^2\delta(\omega_d-\omega_1-\omega_2)$, where the effective Rabi rate is

$$\Omega_{\mathrm{eff}}=\sum_k\left[\frac{\Omega_{gk,1}\Omega_{ke,2}}{\omega_k-\omega_g-\omega_1}+\frac{\Omega_{gk,2}\Omega_{ke,1}}{\omega_k-\omega_g-\omega_2}\right]. \tag{1}$$

The summation is performed over all virtual intermediate states k. $\Omega_{gk,i=1,2}$ ($\Omega_{ke,i}$) is the Rabi transition rate between the ground (intermediate) state and the intermediate (excited) state driven by the laser with frequency ω_i. By substituting the different Rabi rates, we obtain the TPA rates in bulk and double-mode cavity (with resonance frequencies ω_{1c} and ω_{2c}), respectively,

$$\gamma_0^{\mathrm{TPA}}=\frac{\pi}{2}\left[\frac{P_1}{2\hbar^2 n\varepsilon_0 cA_1}\right]\left[\frac{P_2}{2\hbar^2 n\varepsilon_0 cA_2}\right]M_{12}^2\delta(\omega_d-\omega_1-\omega_2),$$

and

$$\gamma_{\omega_{1c},\omega_{2c}}^{\mathrm{TPA}}=\frac{\pi}{2}\left[\frac{\eta_1P_1Q_1\phi_1}{2\hbar^2\omega_1 n^2\varepsilon_0V_1}\right]\left[\frac{\eta_2P_2Q_2\phi_2}{2\hbar^2\omega_2 n^2\varepsilon_0V_2}\right]\times M_{12}^2\delta(\omega_d-\omega_1-\omega_2). \tag{2}$$

In these two expressions, n, ε_0, and c are the refractive index, free space permittivity, and speed of light, respectively. P_i, A_i, and η_i are the power, spot area, and incoupling efficiency of laser beam with frequency ω_i, while Q_i and V_i are the quality factor and mode volume of cavity mode with frequency ω_{ic}. ϕ_i characterizes the frequency mismatch between ω_i and ω_{ic}: $\phi_i=\frac{\omega_i/\omega_{ic}}{1+4Q_i^2(\omega_i/\omega_{ic}-1)^2}$. M_{12} is defined as

$$M_{12}=\left|\sum_k\left[\frac{|\mathbf{d}_{gk}||\mathbf{d}_{ke}|\psi_{gk,1}\psi_{ke,2}}{\omega_k-\omega_g-\omega_1}+\frac{|\mathbf{d}_{gk}||\mathbf{d}_{ke}|\psi_{gk,2}\psi_{ke,1}}{\omega_k-\omega_g-\omega_2}\right]\right|,$$

where $\mathbf{d}_{gk}$ ($\mathbf{d}_{ke}$) is the transition dipole moment between the ground (intermediate) state and the intermediate (excited) state. $\psi_{gk,1}$ characterizes the reduction in Rabi rate due to position mismatch between the QD and the electric field maximum within the cavity: $\psi_{gk,1}=\frac{|\mathbf{E}_1(\mathbf{r})|}{|\mathbf{E}_1(\mathbf{r}_M)|}\left(\frac{\mathbf{d}_{gk}\cdot\mathbf{e}_1}{|\mathbf{d}_{gk}|}\right)$, where $\mathbf{E}_1(\mathbf{r})$ is the electric field at the QD location, $|\mathbf{E}_1(\mathbf{r}_M)|$ is the maximum field strength in the cavity, and $\mathbf{e}_1$ is the polarization of the field. In the nondegenerate TPA, the absorption rate has a linear dependence on P_1 and P_2. In the degenerate case, $\omega_1=\omega_2$ and the absorption rate has a quadratic dependence on power, as expected. In general for the same excitation laser power and laser frequencies resonant with cavity mode frequencies, the rate enhancement is $\gamma_{\omega_{1c},\omega_{2c}}^{\mathrm{TPA}}/\gamma_0^{\mathrm{TPA}}=G_1G_2$, where $G_i=\eta_iQ_iA_i\lambda_i/(\pi V_in)$. Therefore, a single-mode cavity enhances the degenerate TPA by factor which scales as $(Q/V)^2$.

Two-photon excitation of QDs holds several advantages over conventional one-photon excitation. By tuning excitation laser frequencies ω_1 and ω_2 such that their sum matches the quantum-dot transition frequency ω_d, we can coherently excite a QD and therefore create a source of indistinguishable single photons on demand. This is because we eliminate a 10–30 ps time jitter in emitted single photons which results from off-resonant excitation and phonon-assisted carrier decay from the higher excited states to the first excited state.[7] Two-photon excitation also presents a solution for the separation of signal and probe photons in resonant QD excitation because the excitation and emission wavelengths are different. Finally, TPA offers a convenient tool to coherently excite and manipulate a QD for quantum information processing.[20]

B. Two-photon emission

Similarly, for two-photon spontaneous emission (TPSE) [Fig. 1(c)], we compare emission rate $\Gamma_0^{\mathrm{TPSE}}(\omega_1,\omega_2)$ of a QD in bulk semiconductor host with emission rate $\Gamma_{\omega_{1c},\omega_{2c}}^{\mathrm{TPSE}}(\omega_1,\omega_2)$ of a QD in a double-mode cavity centered at ω_{1c} and ω_{2c}

$$\frac{\partial\Gamma_0^{\mathrm{TPSE}}}{\partial\omega_2}=\frac{\pi}{2}\left[\frac{n\omega_1^3}{3\pi^2\hbar\varepsilon_0c^3}\right]\left[\frac{n\omega_2^3}{3\pi^2\hbar\varepsilon_0c^3}\right]M_{12}^2$$

with all ψ's equal 1 and

$$\frac{\partial\Gamma_{\omega_{1c},\omega_{2c}}^{\mathrm{TPSE}}}{\partial\omega_2}=\frac{\pi}{2}\left[\frac{2Q_1\phi_1}{\pi\hbar n^2\varepsilon_0V_1}\right]\left[\frac{2Q_2\phi_2}{\pi\hbar n^2\varepsilon_0V_2}\right]M_{12}^2. \tag{3}$$

Unlike TPA in which one selects the two photon frequencies, QD TPE occurs in a spectrum of (ω_1,ω_2) as long as energy conservation $\omega_1+\omega_2=\omega_d$ is satisfied. Therefore the emission rate is expressed per ω_2 (or ω_1).

Physically, TPSE occurs as the result of the interaction between the excited QD and the vacuum states of the electromagnetic field with modes of frequencies ω_1 and ω_2. As mentioned before, the TPSE spectrum of a single QD is broad because there is a series of (ω_1,ω_2) satisfying energy conservation. Furthermore, the TPSE is slower than the one-photon emission because virtual states are required for it. The combination of broad spectrum and low transition rate results in an overall low signal intensity, and therefore TPSE is generally difficult to detect.

However, the TPSE rate is enhanced when the QD is placed inside a cavity because the cavity modifies the photon density of states in free space into a Lorentzian distribution and also localizes field into small volume which leads to stronger interaction. The TPSE spectrum is thus narrower as it is enhanced around the cavity mode frequencies. The two-photon rate enhancement in a double-mode cavity relative to the bulk medium can be seen by taking the ratio of Eqs. (3)

$$\frac{\Gamma_{\omega_{1c},\omega_{2c}}^{\mathrm{TPSE}}}{\Gamma_0^{\mathrm{TPSE}}}=F_1F_2\quad\text{with}\quad F_i=\frac{3}{4\pi^2}\left(\frac{\lambda_i}{n}\right)^3\frac{Q_i\phi_i}{V_i},$$

where F_i is the Purcell factor[21] and $\lambda_i=2\pi c/\omega_i$, respectively. It should be noted that this expression corresponds to the maximum enhancement, assuming the QD is located at the field maxima for both modes (i.e., all $\psi'\text{s}=1$).

Experimentally, single-mode cavities with Q's exceeding 10^4 and mode volumes below cubic optical wavelength have

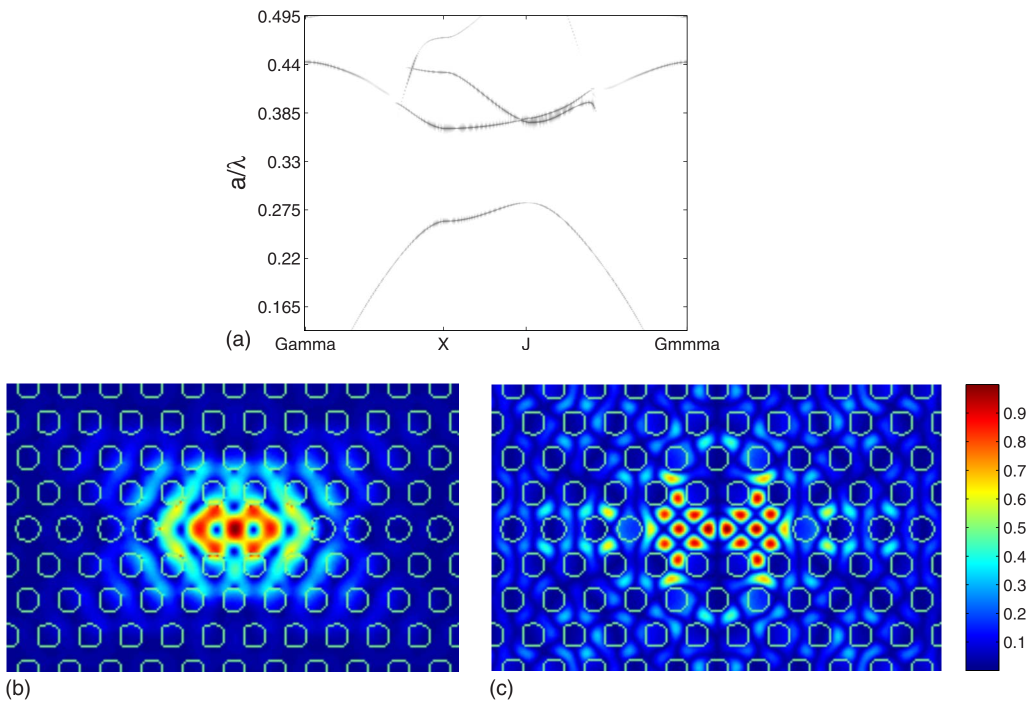

FIG. 2. (Color online) (a) Band diagram for TE-like modes (dominant in-plane electric field) of hexagonal lattice photonic crystal with $r/a=0.30$. (b) Fundamental L3 cavity mode electric field amplitude pattern at frequency $a/\lambda=0.29$. (c) Magnetic field amplitude pattern of the resonance at $a/\lambda=0.43$, obtained by a weak localization of the TE band at Γ point of the band diagram (a) with frequency at $a/\lambda=0.44$.

been demonstrated, and doubly resonant cavities with similar Q's and mode volumes are possible.[22] Therefore, we would expect the maximum TPSE enhancement factor to be 10^4 in single-mode cavities and 10^8 in double-mode cavities. In practice, the single-photon Purcell factor is typically 10–100 owing to the spatial mismatch (ψ's $\neq 1$) and/or the spectral mismatch (ϕ's $\neq 1$).[1] Therefore, we expect the TPSE enhancement to be in the range from 100 to 10^4. Second, in photonic crystal cavities only the emission rates with frequency pair (ω_1,ω_2) matching the cavity frequencies $(\omega_{1c},\omega_{2c})$ are enhanced while emission rates with other frequency pairs are greatly suppressed. Thus, the cavities offer a good control over the frequencies of emitted photons. Third, inside a double-mode cavity with degenerate polarizations for both modes, the two emitted photons are entangled in polarization.

Finally, we derive the two-photon stimulated emission (TPSTE) rate in a double-mode cavity stimulated by a laser beam with power P_2, coupling efficiency η_2, and frequency ω_2

$$\Gamma^{\mathrm{TPSTE}}_{\omega_{1c},\omega_{2c}} = \frac{\pi}{2}\left[\frac{2Q_1\phi_1}{\pi\hbar n^2\varepsilon_0 V_1}\right]\left[\frac{\eta_2 P_2 Q_2\phi_2}{2\hbar^2\omega_2 n^2\varepsilon_0 V_2}\right]M_{12}^2. \qquad (4)$$

Equation (4) shows that the TPSTE rate is linearly dependent on the stimulation laser power and the rate is increased by a factor of $\eta_2 P_2 \pi/(4\hbar\omega_2)$ compared to the TPSE rate. This additional enhancement makes the QD a selective single-photon emitter at ω_1. In other words, if a QD is resonantly excited via one-photon process at ω_d and also driven by a laser with frequency ω_2, it would generate single photons at frequency $\omega_1=\omega_d-\omega_2$.

III. EXPERIMENTAL PROPOSAL

Our system of interest for demonstration of the proposed experiments is an InAs QDs embedded in two-dimensional GaAs PC cavities [Fig. 1(a)]. Consider QDs with s shell-s shell transition wavelength of $\lambda_d=925$ nm. For cavity-enhanced degenerate TPA, the two excitation photons have the same wavelength of 1850 nm. As an example, we choose a linear three-hole defect (L3) cavity with fundamental mode at 1850 nm [Fig. 2(b)] with the following parameters (simulated by finite-difference time-domain method): hexagonal lattice constant $a=537$ nm ($a/\lambda=0.29$), slab thickness $d=242$ nm ($d/a=0.45$), and hole radius $r=161$ nm ($r/a=0.30$). The nearest two holes along the defect are each shifted outward by $s=81$ nm ($s/a=0.15$), which result in a cavity quality factor exceeding 21 000 and a mode volume approximately $0.75(\lambda/n)^3$. This mode locates in the band gap of the photonic crystal band diagram [Fig. 2(a)].

For the proposals we described above, it is important to have a transition that is accessible by both one-photon and two-photon processes. However, two-photon transitions have different selection rule from one-photon transitions. Particularly for QDs, s shell-s shell and p shell-p shell two-photon transitions are forbidden but s shell-p two-photon transitions are allowed due to parity. To achieve two-photon s shell-s shell transitions, we propose the application of lateral electric fields to break the parity symmetry in wave functions [Figs.

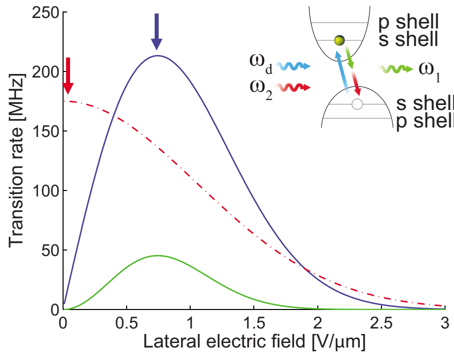

FIG. 3. (Color online) Cavity-enhanced two-photon absorption effective Rabi rate (blue solid line), enhanced one-photon spontaneous emission rate (red dash-dot line), and 100× two-photon stimulated emission rate (green solid line) as a function of lateral electric field strength. All of the transitions are *s* shell-*s* shell. The simulation parameters are shown in text. Inset: illustration of two-photon stimulated emission.

1(b) and 1(c)]. Recent experiments have demonstrated the Stark shift of QD transitions in bulk[23] as well as in photonic crystal cavities.[24,25] Following Refs. 23 and 26, we model the QD as a particle in a finite well along its growth axis and a two-dimensional harmonic oscillator perpendicular to its growth axis. We denote the electron (hole) effective mass and oscillator frequency as m_e^* and ω_e (m_h^* and ω_h). For the one-photon *s* shell-*s* shell transition, the lateral electric field $\mathcal{E}$ reduces this transition dipole moment with expression $\mathbf{d}_{ge}=e\mathbf{r}_{cv}\exp[-(\Delta x)^2/(4l_e^2)]$, where $\mathbf{r}_{cv}$ is the transition moment between the valence and the conduction bands, $\Delta x=e\mathcal{E}[(m_e^*\omega_e^2)^{-1}+(m_h^*\omega_h^2)^{-1}]$ is the separation of the electron and hole wave-function centers, and $l_e=l_h=\sqrt{\hbar/(2m_e^*\omega_e)}$ is the oscillator length. For the two-photon *s* shell-*s* shell transition, the predominant intermediate states are the conduction and valence *p* shell states. Assuming $|k\rangle$=conduction *p* shell, we have $|\mathbf{d}_{gk}|=e|\mathbf{r}_{cv}|(\Delta x/l_e)\exp[-(\Delta x)^2/(4l_e^2)]$, $|\mathbf{d}_{ke}|=el_e$, and therefore $|\mathbf{d}_{gk}||\mathbf{d}_{ke}|=e^2|\mathbf{r}_{cv}|\Delta x\exp[-(\Delta x)^2/(4l_e^2)]$. The case of $|k\rangle$=valence *p* shell gives the same product of transition dipole moments.

Figure 3 shows the enhanced degenerate TPA effective Rabi rate $\Omega_{\text{eff}}/2\pi$ [Eq. (1)] and one-photon spontaneous emission rate $\Gamma^{\text{OPSE}}/2\pi$ as a function of lateral electric field. The simulation parameters are $m_h^*=2m_e^*=0.11m_0$ (m_0 is the electron rest mass), $\hbar\omega_e=2\hbar\omega_h=12$ meV,[26] and $|\mathbf{r}_{cv}|=0.6$ nm.[27] We use conservative parameters of $Q_1=Q_2=10^4$, $V_i=0.75(\lambda_i/n)^3$, $\phi'\text{s}=0.5$, and $\psi'\text{s}=0.5$ (corresponding a QD-cavity spectral mismatch of half cavity line width). A QD positioned in a 925 nm cavity with these parameters experiences a Purcell enhancement of 31. A continuous-wave laser light with wavelength of 1850 nm and power of $P_1=P_2=10$ μW is coupled into the cavity with efficiency $\eta_1=\eta_2=5\%$. The assumed low incoupling efficiencies are taken from the experiments where the input laser beam is coupled to the cavity in the direction perpendicular to the chip.[6,28] However, it must be pointed out that PC cavities coupled to fiber tapers or PC waveguide can achieve a coupling efficiency of 70–90 % (Refs. 29 and 30) and therefore reduce the needed external excitation power. For enhanced TPA and subsequent single-photon generation, we operate in the region where $\mathcal{E}<0.5$ V/μm with $\Omega_{\text{eff}}<\Gamma^{\text{OPSE}}$ to prevent Rabi oscillations between the ground and excited states.

In addition to the application of a static electric field, a modulation of electric field can change the parity selection rules dynamically. For example, we can keep the electric field on at approximately 0.75 V/μm to enable the *s* shell-*s* shell excitation via TPA (Fig. 3 blue arrow) but then turn off the field to permit a rapid single-photon emission (Fig. 3 red arrow). This way we can achieve maximum transitions rates in both excitation and photon emission. For an estimation of the modulation speed, we need to switch the electric field on a time scale that is faster than the recombination rate for an excited QD, which is 100 ps to 1 ns. Today's commercial function generators can easily achieve this speed.

For a QD inside a cavity with the parameters given above, the total two-photon spontaneous emission rate reaches its maximum of 16 kHz at $\mathcal{E}=0.75$ V/μm, which might be detected by lock-in amplification. To demonstrate two-photon stimulated emission, the photon frequencies need to be nondegenerate. We select two-photon wavelengths as $\lambda_1=1550$ nm and $\lambda_2=2300$ nm, conveniently coinciding with the telecom band (suitable for propagation down the fiber) and emission from existing GaSb lasers, respectively. We scale up our L3 cavity design mentioned in the previous paragraph and choose hexagonal lattice constant $a=667$ nm, slab thickness $d=300$ nm, and hole radius $r=200$ nm to achieve a fundamental mode [Fig. 2(b)] resonance at 2300 nm with a quality factor of 21 000. The other mode at 1550 nm is a guided resonance with $a/\lambda=0.43$, quality factor $Q\sim200$, and mode volume $V=6.4(\lambda/n)^3$ [Fig. 2(c)]. This guided resonance locates at the TE band at the Γ point of the band diagram [Fig. 2(a)]. Figure 3 shows the cavity-enhanced TPSTE rate of 1550 nm photons as a function of lateral electric field calculated with these parameters. The maximum emission rate occurs at $\mathcal{E}=0.75$ V/μm. Although the emission rate is below 1 MHz, we emphasize that this signal might be detected by lock-in amplification and that the 925 nm single photons emitted by the QD do not serve as a background for the TPE detection due to wavelength difference.

IV. CONCLUSION

We have derived the expressions for enhancement of two-photon absorption, two-photon spontaneous emission, and two-photon stimulated emission from a single QD in an optical nanocavity. We have presented a simple cavity design to achieve QD degenerate two-photon absorption with power as low as 10 μW. This allows us to employ enhanced two-photon absorption to coherently excite quantum dots and enable generation of indistinguishable single photons on demand. We have also presented a design to achieve enhanced nondegenerate two-photon emission, which can be employed to generate single photons.

Although we focus on semiconductor QDs as an illustration for cavity-enhanced TPA and TPE in this paper, we can use the same approach to excite and manipulate other emitters such as 637 nm nitrogen-vacancy centers by laser beams in the 1550 nm telecom range. The cavity-enhanced TPA and TPE can even enable construction of hybrid quantum networks containing different emitters just by changing the frequency of one of the excitation lasers.

ACKNOWLEDGMENTS

The authors gratefully acknowledge financial support provided by National Science Foundation and the Army Research Office.

---

*carterlin@stanford.edu

[1] D. Englund, A. Faraon, B. Zhang, Y. Yamamoto, and J. Vuckovic, Opt. Express **15**, 5550 (2007).

[2] S. Laurent, S. Varoutsis, L. L. Gratiet, A. Lemaître, I. Sagnes, F. Raineri, A. Levenson, I. Robert-Philip, and I. Abram, Appl. Phys. Lett. **87**, 163107 (2005).

[3] D. Englund, D. Fattal, E. Waks, G. Solomon, B. Zhang, T. Nakaoka, Y. Arakawa, Y. Yamamoto, and J. Vuckovic, Phys. Rev. Lett. **95**, 013904 (2005).

[4] K. Hennessy, A. Badolato, M. Winger, D. Gerace, M. Atature, S. Gulde, S. Falt, E. L. Hu, and A. Imamoglu, Nature (London) **445**, 896 (2007).

[5] T. Yoshie, A. Scherer, J. Hendrickson, G. Khitrova, H. M. Gibbs, G. Rupper, C. Ell, O. B. Shchekin, and D. G. Deppe, Nature (London) **432**, 200 (2004).

[6] D. Englund, A. Faraon, I. Fushman, N. Stoltz, P. Petroff, and J. Vuckovic, Nature (London) **450**, 857 (2007).

[7] J. Vuckovic, D. Englund, D. Fattal, E. Waks, and Y. Yamamoto, Physica E (Amsterdam) **32**, 466 (2006).

[8] C. Becher, A. Kiraz, P. Michler, W. V. Schoenfeld, P. M. Petroff, L. Zhang, E. Hu, and A. Imamoglu, Physica E (Amsterdam) **13**, 412 (2002).

[9] C. Santori, D. Fattal, J. Vuckovic, G. S. Solomon, and Y. Yamamoto, Nature (London) **419**, 594 (2002).

[10] S. Ates, S. M. Ulrich, S. Reitzenstein, A. Loffler, A. Forchel, and P. Michler, Phys. Rev. Lett. **103**, 167402 (2009).

[11] O. Benson, C. Santori, M. Pelton, and Y. Yamamoto, Phys. Rev. Lett. **84**, 2513 (2000).

[12] D. Gammon, E. S. Snow, B. V. Shanabrook, D. S. Katzer, and D. Park, Phys. Rev. Lett. **76**, 3005 (1996).

[13] M. Bayer, G. Ortner, O. Stern, A. Kuther, A. A. Gorbunov, A. Forchel, P. Hawrylak, S. Fafard, K. Hinzer, T. L. Reinecke, S. N. Walck, J. P. Reithmaier, F. Klopf, and F. Schäfer, Phys. Rev. B **65**, 195315 (2002).

[14] N. Akopian, N. H. Lindner, E. Poem, Y. Berlatzky, J. Avron, D. Gershoni, B. D. Gerardot, and P. M. Petroff, Phys. Rev. Lett. **96**, 130501 (2006).

[15] R. M. Stevenson, R. J. Young, P. Atkinson, K. Cooper, D. A. Ritchie, and A. J. Shields, Nature **439**, 179 (2006).

[16] A. Hayat, P. Ginzburg, and M. Orenstein, Nat. Photonics **2**, 238 (2008).

[17] L. A. Padilha, J. Fu, D. J. Hagan, E. W. Van Stryland, C. L. Cesar, L. C. Barbosa, C. H. B. Cruz, D. Buso, and A. Martucci, Phys. Rev. B **75**, 075325 (2007).

[18] G. Xing, W. Ji, Y. Zheng, and J. Y. Ying, Appl. Phys. Lett. **93**, 241114 (2008).

[19] R. W. Boyd, *Nonlinear Optics*, 2nd ed. (Academic, New York, 2003).

[20] D. Englund, A. Majumdar, A. Faraon, M. Toishi, N. Stoltz, P. Petroff, and J. Vuckovic, arXiv:0902.2428 (unpublished).

[21] E. M. Purcell, Phys. Rev. **69**, 681 (1946).

[22] J. Vuckovic, M. Loncar, H. Mabuchi, and A. Scherer, Phys. Rev. E **65**, 016608 (2001).

[23] M. E. Reimer, M. Korkusinski, D. Dalacu, J. Lefebvre, J. Lapointe, P. J. Poole, G. C. Aers, W. R. McKinnon, P. Hawrylak, and R. L. Williams, Phys. Rev. B **78**, 195301 (2008).

[24] A. Faraon, A. Majumdar, H. Kim, P. Petroff, and J. Vuckovic, arXiv:0906.0751 (unpublished).

[25] A. Laucht, F. Hofbauer, N. Hauke, J. Angele, S. Stobbe, M. Kaniber, G. Bohm, P. Lodahl, M.-C. Amann, and J. J. Finley, New J. Phys. **11**, 023034 (2009).

[26] M. Korkusinski, M. E. Reimer, R. L. Williams, and P. Hawrylak, Phys. Rev. B **79**, 035309 (2009).

[27] P. G. Eliseev, H. Li, A. Stintz, G. T. Liu, T. C. Newell, K. J. Malloy, and L. F. Lester, Appl. Phys. Lett. **77**, 262 (2000).

[28] A. Faraon, I. Fushman, D. Englund, N. Stoltz, P. Petroff, and J. Vuckovic, Nat. Phys. **4**, 859 (2008).

[29] I.-K. Hwang, S.-K. Kim, J.-K. Yang, S.-H. Kim, S. H. Lee, and Y.-H. Lee, Appl. Phys. Lett. **87**, 131107 (2005).

[30] A. Faraon, E. Waks, D. Englund, I. Fushman, and J. Vuckovic, Appl. Phys. Lett. **90**, 073102 (2007).